Journal of Network and Innovative Computing
ISSN 2160-2174 Volume 3 (2015) pp. 019-028

Optimal design of concentric hexagonal array antenna using Improved Particle Swarm Optimization technique

Rajesh Bera[1], Durbadal Mandal[1], Sakti Prasad Ghoshal[2], Rajib Kar[1]

[1]Department of Electronics and Communication Engineering,
National Institute of Technology Durgapur, West Bengal, India
{rajeshkiit12, durbadal.bittu, rajibkarece}@gmail.com

[2]Department of Electrical Engineering,
National Institute of Technology Durgapur, West Bengal, India
spghoshalnitdgp@gmail.com

***Abstract*: In this paper, the optimal design of two-ring Concentric Hexagonal Array (CHA) of uniformly excited isotropic antennas which can generate directive beam with minimum relative Side Lobe Level (SLL) is described. The Improved Particle Swarm Optimization (IPSO) method, which represents a new approach for optimization problems in electromagnetics, is applied for the optimization process. To improve the radiation pattern with maximum SLL reduction, an optimum set of antenna parameters as excitation weights and ring spacing of the CHA are to be developed. Three design examples are presented that illustrate the effectiveness of the IPSO algorithm, and the optimization goal in each example is easily achieved. In the first example, optimal thinning of 24-element CHA with maximum SLL reduction is presented. In second and third examples, IPSO technique is used to determine an optimal set of non-uniformly excited array of 24 and 30 elements, respectively that provide a radiation pattern with maximum SLL reduction. Results clearly show the superiority of the IPSO over PSO to handle the proposed problem.**

***Keywords*:** Thinned array, particle swarm optimization, improved particle swarm optimization, concentric hexagonal array, side lobe level.

I. Introduction

In many applications, to meet the requirements of long distance communication, it is necessary to design antennas with very high directive characteristics. This can be achieved by shaping an assembly of radiating elements in electrical and geometrical arrangement, which is referred to as an array. Antenna arrays have been widely used in different applications including direction finding, scanning, radar, sonar, and wireless communications [1]. They are useful in high power transmission, low power consumption and enhanced spectral efficiency. To provide a very high directive pattern, it is necessary that the fields from the array elements must add constructively in some desired directions and add destructively and cancel each other in the remaining space. Interference from the undesired directions can be reduced by reducing the side lobes of the antenna.

In wireless communication, one of the most recent innovations to overcome the problem of increasing demand for capacity is to deploy smart antenna [2]. Smart antenna can be visualized as the antenna directing a beam toward the communication partner only. Smart antennas not only increase the capacity, they have also adaptability to introduce new services, increased range, more security, reduced multipath propagation etc. Narrower main-beam and large number of nulls in the pattern can resolve the Signals-Of-Interest (SOI) more accurately and allow the smart antenna system to reject more Signals-Not-Of-Interest (SNOI).

A linear array has excellent directivity and it can form the narrowest main-lobe in a given direction, but it does not work well in all azimuth directions. Since a circular array does not have edge elements, directional patterns synthesized with a circular array can be electronically rotated in the plane of the array without a significant change of the beam shape [3]. And, circular array pattern has no nulls in azimuth plane [1]. In smart antenna applications to reject SNOI the array pattern should have several nulls in the azimuth plane. This can be implemented by the use of elliptical arrays instead of circular arrays [4].

The circular array is of high side-lobe geometry. If the distance of array elements is decreased to reduce the side lobes, the mutual coupling influence becomes more significant. For mitigating high side-lobe levels, concentric arrays are utilized. Also concentric circular array antennas have several advantages including the flexibility in array pattern synthesis and design both in narrowband and broadband beam forming applications [5].

Array thinning involves the removal (switching off) of some radiating elements from a uniformly spaced or periodic array antenna to generate a pattern with low SLL. In this method, the locations of the elements are fixed and all the elements have two states either “on”(active) or “off”(removed) depending on whether the element is connected to the feed network or not. All the active elements are fed with equal amplitude currents,

while the remaining elements are turned off. In the "off" state, either the element is passively terminated to a matched load or open-circuited. It is equivalent to removing elements from array if there is no coupling between them. The main objectives of array thinning are reduction of cost, weight and power consumption where the performance of array is not significantly degraded. There are many published articles [6]-[8] dealing with the synthesis of array thinning.

The null steering of linear antenna arrays by controlling the element amplitudes has been discussed in [9].

The design of nonuniform circular antenna arrays for maximum reduction of side lobe level and first null beam width using Firefly algorithm (FFA) has been presented in [10].

In [11], the comparison between circular array and hexagonal array shows that hexagonal array geometries give slightly deeper nulls, higher gain and a smaller overall size, with the same beam width as circular array geometries.

In [12], artificial bee colony (ABC) optimization and firefly algorithm (FA) have been applied to synthesize beam patterns of a hexagonal planar array of isotropic elements.

Thinning of elliptical antenna arrays using PSO is optimized with different values of eccentricity and variation of side lobe level with eccentricity of thinned antenna array is reported in [13].

There are several disadvantages when using classical optimization methods. Some of them are: i) when the number of solution variables i.e. the size of the solution space increases, starting point is highly sensitive because the solution of an optimization problem solved using a classical method depends on the arbitrarily chosen initial solution, ii) requirement of continuous and differentiable objective functions because discrete variables are difficult to handle using classical methods of optimization, iii) a particular classical optimization method may not be appropriate to solve various problems, etc. Thus, it is necessary to develop an efficient and robust optimization method. There are various evolutionary optimization techniques such as Genetic Algorithm (GA) [8], Particle Swarm Optimization (PSO) [14]-[19], Ant Colony Optimization (ACO) etc. for optimization of complex, highly nonlinear, discontinuous and non-differentiable array factor of antenna array, which do not suffer from above disadvantages.

II. Design Equation

The total field of an array, according to pattern multiplication principle, can be formed by multiplying the field of a single element at a selected reference point and the array factor. The array factor can be formulated by replacing the actual elements with isotropic (point) sources. The array factor of an array in general can be written as (1) [1].

$$AF(\theta,\varphi)=\sum_{n=1}^{N}A_n e^{j(\alpha_n+kR_n.a_r)} \tag{1}$$

where N is the number of elements, A_n is the relative amplitude of *n-th* element, α_n is the relative phase of *n-th* element, R_n is the position vector of *n-th* element depends on array geometry, a_r is the unit vector of observation point in spherical coordinate and k is the wave number.

The array factor of an N-element circular array (CA) with its center in origin of $x-y$ plane, is [3]

$$AF(\theta,\varphi)=\sum_{n=1}^{N}A_n e^{jkr\sin\theta(\cos\varphi_n\cos\varphi+\sin\varphi_n\sin\varphi)} \tag{2}$$

where r is radius of the circle, ϕ is the angle between positive section of x axis and the observation point in the space, θ is the angle between positive section of z axis and the observation point in the space, $2\pi(n-1)/N$ is the angle in the $x-y$ plane between the x axis and the n-th element.

The hexagonal array (HA) which the peripheral curve of its vertices is a circle can be treated as consisting of two concentric N-element circular arrays of different radii r_1 and r_2, respectively. Fig. 1 gives a simple example of hexagonal array with $2N$ elements ($N = 6$), N of which are located at the vertices of the hexagon and the other N elements are placed at the middle of each line of the hexagon, respectively. Using (2) and above explanation, the array factor of hexagonal array is

$$AF(\theta,\varphi)=\sum_{n=1}^{N}[A_n e^{jkr_1\sin\theta(\cos\varphi_{1n}\cos\varphi+\sin\varphi_{1n}\sin\varphi)} + B_n e^{jkr_2\sin\theta(\cos\varphi_{2n}\cos\varphi+\sin\varphi_{2n}\sin\varphi)}] \tag{3}$$

$$r_2=r_1\cos(\pi/N),\quad r_1=d/\sin(\pi/N) \tag{4}$$

where $\varphi_{1n}=2\pi(n-1)/N$ is the angle in the x-y plane between the x axis and the n th element at the vertices of the hexagon, $\varphi_{2n}=\varphi_{1n}+\pi/N$ is the angle in the x−y plane between the x axis and the n-th element at the middle of each line of the hexagon, A_n, B_n are the relative amplitudes of n-th element placed at the vertices and the middle of the hexagon, respectively, d is the spacing between two elements in the inner-most ring.

The array factor of concentric hexagonal array (CHA), as shown in Fig. 2, can be found by summation of the array factors of M concentric HA.

$$AF(\theta,\varphi)=\sum_{m=1}^{M}\sum_{n=1}^{N}[A_{nm}e^{jkr_{1m}\sin\theta(\cos\varphi_{1n}\cos\varphi+\sin\varphi_{1n}\sin\varphi)} + B_{nm}e^{jkr_{2m}\sin\theta(\cos\varphi_{2n}\cos\varphi+\sin\varphi_{2n}\sin\varphi)}] \tag{5}$$

where 2N is the number of elements on each hexagon, M is the number of concentric hexagons, A_{nm} , B_{nm} are the amplitudes of excitation currents, r_{1m} is the radius of the circle on which elements are placed at the vertices of the m-th hexagon. r_{2m} is the radius of the circle on which elements are placed at the middle of each line of the *m-th* hexagon.

$$r_{1m}=r+(m-1)d_h$$
$$r_{2m}=r_{1m}\cos(\pi/N) \tag{6}$$

where r is the radius of smallest circle peripheral to the smallest hexagon whose elements lie on its vertices and d_h is the spacing between hexagons along X-axis.

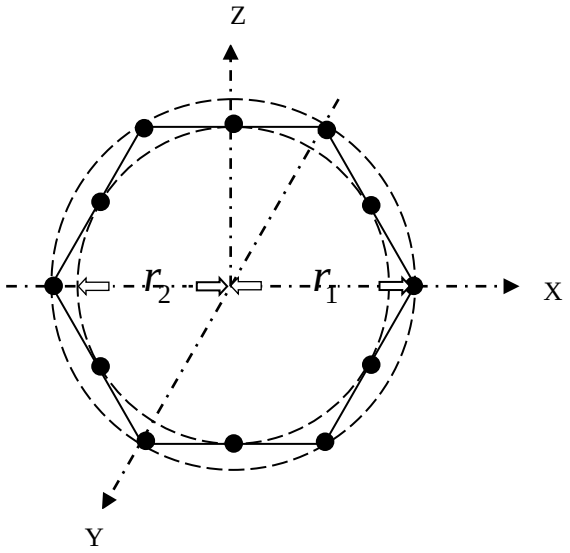

Figure 1. Hexagonal Array (HA) Structure.

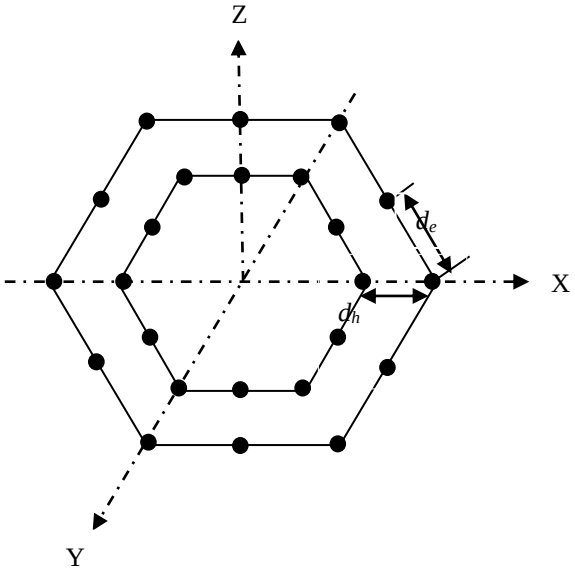

Figure 2. Concentric Hexagonal Array (CHA) Structure.

III. Improved Particle Swarm Optimization

Unlike traditional optimization methods, PSO is a flexible, robust population-based stochastic optimization technique, which can easily handle with non-differential objective functions. The details of PSO are not given as some references on PSO are given in [14]-[19].

Mathematically, velocities of the particles are modified according to the following equation:

$$V_i^{k+1} = w*V_i^k + C_1*rand_1*\left(pbest_i^k - S_i^k\right) + C_2*rand_2*\left(gbest^k - S_i^k\right) \quad (7)$$

where V_i^k = velocity of i[th] particle at k[th] iteration; w= weighting function; C_1 and C_2 are the positive weighting factors; $rand_1$ and $rand_2$ are the random numbers between 0 and 1; S_i^k = current position of the i[th] particle at the k[th] iteration; $pbest_i^k$ = personal best of the i[th] particle at the k[th] iteration; $gbest^k$ = group best of the group at the k[th] iteration. The searching point in the solution space may be modified by the following equation:

$$S_i^{(k+1)} = S_i^k + V_i^{(k+1)} \quad (8)$$

The global search ability of basic PSO is very much enhanced with the help of the following modifications. This modified PSO is termed as IPSO [20]-[22]. Steps of IPSO are not described, only important equations are considered.

With all modifications, the modified velocity of the i[th] particle vector at the (k+1)[th] iteration is expressed as follows:

$$V_i^{(k+1)} = r_2*sign(r_3)*V_i^k + (1-r_2)*C_1*r_1 * \left\{pbest_i^k - S_i^k\right\} + (1-r_2)*C_2*(1-r_1)*\left\{gbest^k - S_i^k\right\} \quad (9)$$

where r_1, r_2 and r_3 are the random numbers between 0 and 1 and $sign(r_3)$ is a function defined as:

$$sign(r_3) = -1 \quad \text{when} \quad r_3 \le 0.05,$$
$$= 1 \quad \text{when} \quad r_3 > 0.05. \quad (10)$$

The searching point in the solution space can be modified by (8).

The first and most important parameter in antenna pattern synthesis is the normalized side lobe level that is desired to be as low as possible. Cost Function (*CF*) is formulated to meet the corresponding design goal as follows:

$$CF = C_1[SLL_c - SLL_d] + C_2[FNBW_c - FNBW_d] \quad (11)$$

where SLL_d and SLL_c are the desired and computed values of SLL, respectively, and $FNBW_d$ and $FNBW_c$ are the desired and computed values of FNBW, respectively. The first term in (11) is used to reduce the SLL to a desired level. The second term in (11) is introduced to keep FNBW of the optimized pattern to a desired level. In (11), SLL_c and SLL_d refer to the computed SLL for the uniform excitation (I_n=1) case and the desired value of SLL for non-uniform excitation case, respectively. Similarly, the two beamwidths $FNBW_c$ and $FNBW_d$ refer to the computed FNBW for the uniform excitation (I_n=1) case and the desired value of FNBW for non-uniform excitation case, respectively. C1 and C2 are weighting coefficients to control the relative importance of each term in (11). Because the primary aim is to achieve a minimum SLL, the value of C1 is higher than the value of C2. The minimum CF values against number of iteration cycles are recorded to get the convergence profile of the algorithm.

IV. Computational Results

In order to present the performances of PSO and IPSO, three different design examples have been considered.

In the first example, optimal thinning of 24- element CHA with maximum SLL reduction is presented. Here, IPSO is employed to determine an optimal set of 'ON-OFF' elements in order to get an array that provides a radiation pattern with maximum SLL reduction. For all design examples, cost

function *CF* is used for the synthesis of the array using the both algorithms. The value of wave number *k* in (5) is chosen 6.75. Figure 2 is a diagram of a 24-element CHA. In CHA, two rings each having 12 elements are considered for synthesis. Here three cases are considered for three different values of inter-ring spacing (d_h) along X-axis in the array. In the first case, spacing between hexagons in CHA is 0.5λ. Similarly, for the second and third cases, spacing are 0.55λ and 0.6λ respectively.

The inter-element spacing of inner ring is kept fixed at d=λ/2 for all the three cases. Calculated values of inter-element spacing for all rings in CHA are tabulated in Table I for the three different cases.

Performances of optimized thinned array antennas with variation of spacing between hexagons are tabulated in Table II. The optimal excitation amplitudes for the thinned CHA using PSO and IPSO are shown in Table III.

Figures 3-5 show the array patterns found by PSO and IPSO for 2 rings CHA and comparison of them with fully populated array pattern.

The following observations are made from Table II, Table III and Figures 3, 4, 5. The algorithms yield SLL values of -20.14dB (PSO) and -22.96dB (IPSO) for the inter-ring spacing 0.5λ, then, -17.23dB (PSO) and -22.88dB (IPSO) for the inter-ring spacing 0.55λ, and finally, -18.05dB (PSO) and -22.01dB (IPSO) for the inter-ring spacing 0.6λ. Further, the above improvement is achieved for an array of high percentage of elements turned off for both the PSO and IPSO.

Distributions of ON and OFF elements of optimized thinned array for various cases are tabulated in Table III. The corresponding array geometries are shown in Figures 6-8.

Thinning is the ratio of the number of 'OFF' elements to the total number of elements in the array.

Table I: Element spacing and number of elements per ring for a three ring CHA.

		Inter-ring spacing d_h (λ)			Total number of elements
		Case 1 d_h=0.5 λ	Case 2 d_h=0.55 λ	Case 3 d_h=0.6 λ	
Inter-element spacing d_e(λ) in CHA	1st ring	0.5	0.5	0.5	24
	2nd ring	0.75	0.775	0.80	24

Table II: thinned and fully populated array results for PSO and IPSO.

Inter-ring spacing d_h(λ)	Thinned array(PSO)		Thinned array(IPSO)		Fully populated array	
	Maximum SLL(dB)	Number of 'ON' elements	Maximum SLL(dB)	Number of 'ON' elements	Maximum SLL(dB)	Number of 'ON' elements
0.50	-20.14	18	-22.96	17	-12.05	24
0.55	-17.23	17	-22.88	18	-12.66	24
0.60	-18.05	10	-22.01	11	-13.33	24

Table III: Excitation amplitude distribution using PSO and IPSO.

Inter-ring spacing d_h(λ)	Ring number	Placement of elements	Distribution of ON and OFF elements	
			PSO	IPSO
0.50	Ring 1	vertices	1 1 1 1 0 0	1 1 0 1 0 1
		middle	1 0 1 1 1 1	1 1 1 1 0 1
	Ring 2	vertices	1 1 0 1 0 1	1 0 1 1 0 1
		middle	1 1 0 1 1 1	1 1 1 0 0 1
0.55	Ring 1	vertices	1 1 1 1 0 1	1 0 1 1 0 0
		middle	1 0 0 1 0 0	1 1 1 1 1 1
	Ring 2	vertices	1 0 1 1 1 0	1 0 1 1 1 0
		middle	1 1 1 1 1 1	1 1 0 1 1 1
0.60	Ring 1	vertices	1 0 0 0 1 0	0 1 0 1 0 0
		middle	1 1 0 0 0 1	1 0 0 0 1 1
	Ring 2	vertices	1 0 0 0 0 1	1 1 0 1 0 1
		middle	1 1 0 0 0 1	1 0 0 1 0 0

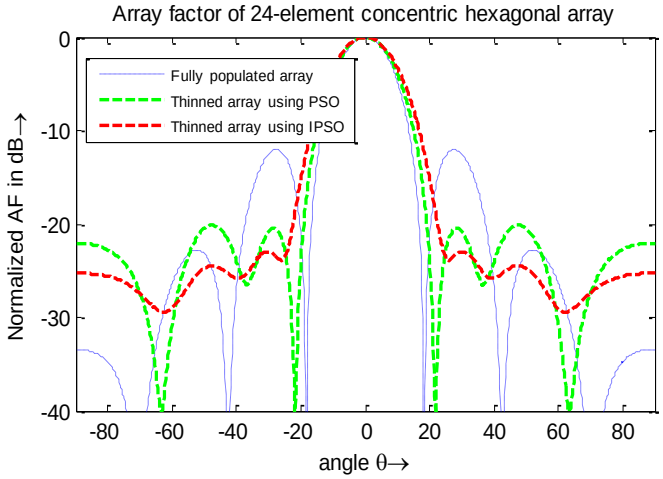

Figure 3. Normalized absolute power patterns for optimized thinned array with fixed inter-ring spacing d_h=0.5λ.

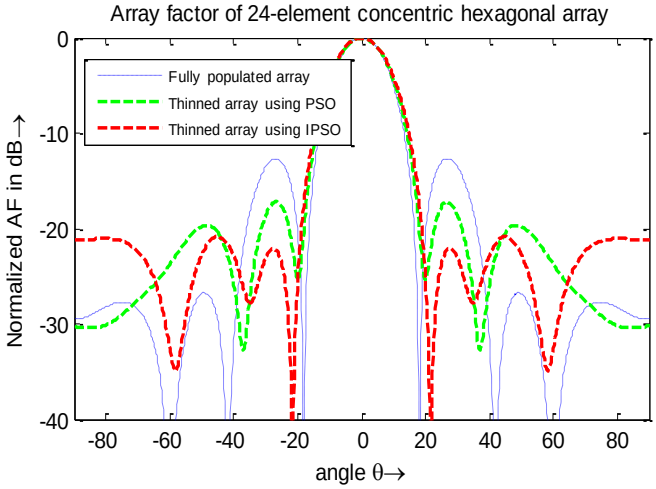

Figure 4. Normalized absolute power patterns for optimized thinned array with fixed inter-ring spacing d_h=0.55λ.

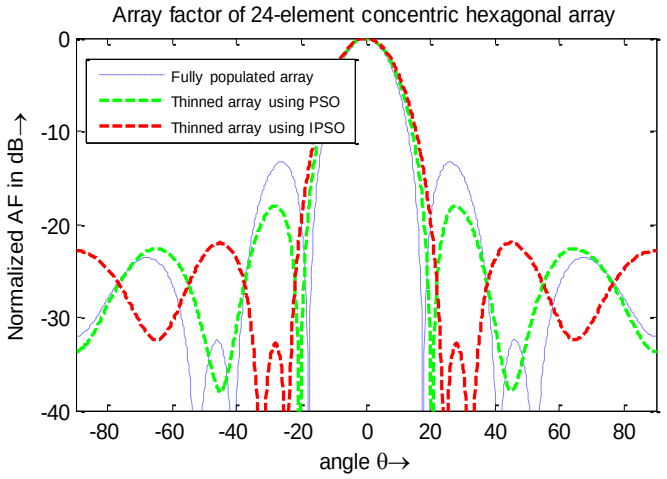

Figure 5. Normalized absolute power patterns for optimized thinned array with fixed inter-ring spacing d_h=0.60λ.

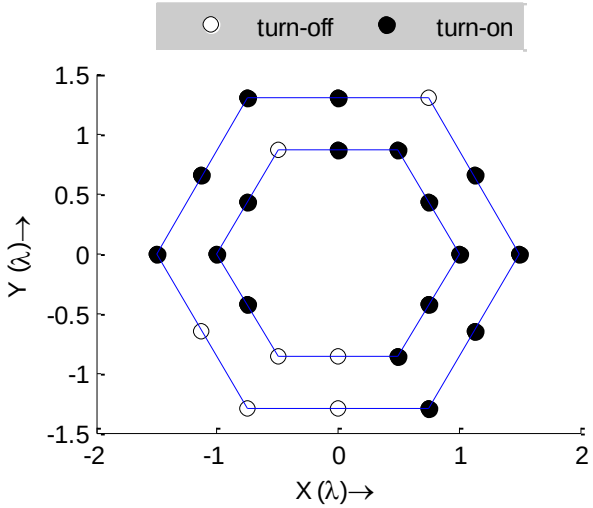

Figure 6. Array geometry for distribution of ON and OFF elements using IPSO when d_h=0.5λ in Table III.

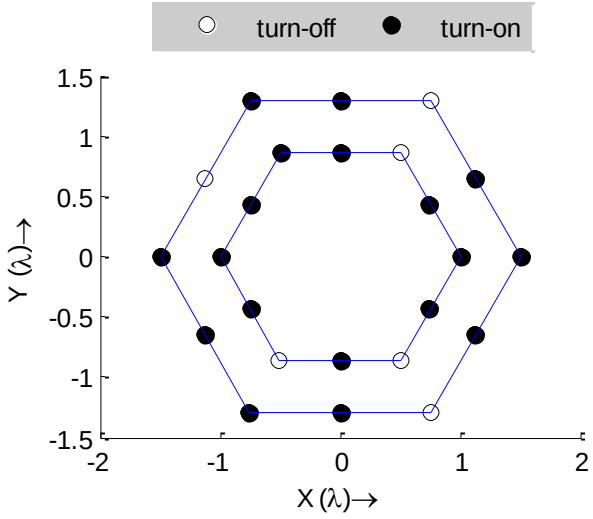

Figure 7. Array geometry for distribution of ON and OFF elements using IPSO when d_h=0.55λ in Table III.

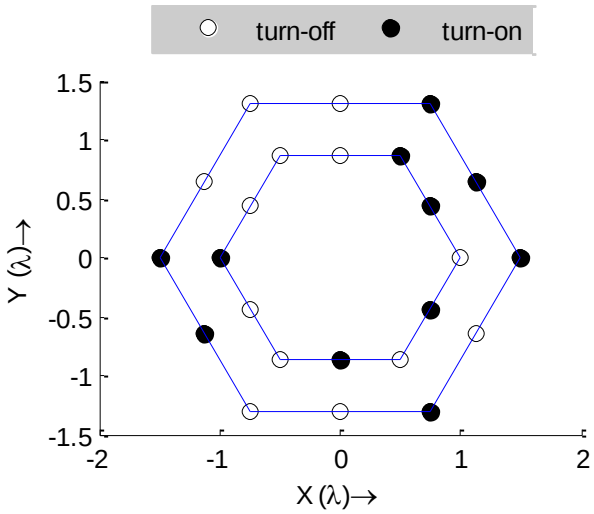

Figure 8. Array geometry for distribution of ON and OFF elements using IPSO when d_h=0.6λ in Table III.

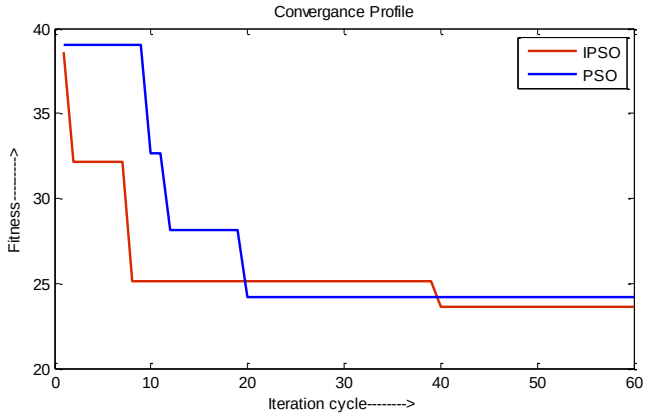

Figure 9. Convergence profile for a 24-element thinned CHA using PSO and IPSO.

Both the algorithms were run for 60 iterations and number of particles in both the cases were taken to be 30. The minimum *CF* values were recorded against number of Iteration cycles to get the convergence profiles for the algorithms. Figure 9 shows that the convergence rate of IPSO is better than PSO for minimizing the cost while thinning the array.

In the second example, optimal design of 24- element CHA with amplitude only optimization is presented. IPSO technique is used to determine an optimal set of non-uniformly excited array that provides a radiation pattern with maximum SLL reduction.

In this example, CHA of two concentric rings each having 12 elements is considered for synthesis. Here also three cases are considered for three different values of inter-ring spacing (d_h) along X-axis in the array. In the first case, spacing between hexagons in CHA is 0.5λ. Similarly, for the second and third cases, spacing are 0.55λ and 0.6λ respectively. The inter-element spacing of inner ring is kept fixed at d=λ/2 for all the three cases.

Performances of 24-element amplitudes only optimized array with variation of spacing between hexagons are tabulated in Table IV. The optimal excitation amplitudes for this CHA using PSO and IPSO are shown in Table V and Table VI, respectively. Figures 10-12 show the array pattern found by PSO and IPSO for various inter-ring spacing of

24-element CHA and comparison of them with fully populated array pattern.

The population size using each algorithm (PSO and IPSO) by which the antenna array is optimized is 50 and maximum number of iteration cycles is 100. The minimum *CF* values are recorded against number of iteration cycles to get the convergence profiles for each algorithm, which is shown in Figure 13.

Table IV: Performances of 24-element CHA using PSO and IPSO

Inter-ring spacing $d_h(\lambda)$	SLL		FNBW	
	PSO	IPSO	PSO	IPSO
0.50	-38.02	-40.03	60.2	62.8
0.55	-35.30	-36.22	56.0	57.2
0.60	-30.98	-32.00	50.4	51.2

Table V: Excitation amplitude distribution of 24-element CHA using PSO

Inter-ring spacing $d_h(\lambda)$	Ring number	Placement of elements	Amplitude distribution
0.50	Ring 1	vertices	1.0000 0.6330 0.0006 0.9985 0.2545 0.4235
		middle	1.0000 0 0.1307 0.3471 0.0026 0.7989
	Ring 2	vertices	0.6797 0 0.2371 0.9860 0.6821 0.1031
		middle	0.8796 0.7492 1.0000 1.0000 0.0040 0.6265
0.55	Ring 1	vertices	0.5735 0.1588 0.3628 0.9994 0.0092 0.4609
		middle	0.5402 0.4685 0.8918 0.8345 0.3949 0.5112
	Ring 2	vertices	0.9919 0.6104 0.0028 0.9981 0.1212 0.7628
		middle	0.7676 0.3752 0.6722 0.7684 0.0647 0.7281
0.60	Ring 1	vertices	0.6611 0.3265 0.6903 0.9206 0.5327 0.4916
		middle	0.3946 0.0004 1.0000 0.9016 0.2808 0.6319
	Ring 2	vertices	0.6929 0.5494 0.1636 0.9971 0.3925 0.3880
		middle	0.7564 0.3103 0.4915 0.2801 0.3445 0.7929

Table VI: Excitation amplitude distribution of 24-element CHA using IPSO

Inter-ring spacing $d_h(\lambda)$	Ring number	Placement of elements	Amplitude distribution
0.50	Ring 1	vertices	0.2826 0.3614 0.0069 0.9779 0 0
		middle	0.5307 0.3890 0.7437 0.2302 0.6615 0.9801
	Ring 2	vertices	0.9840 0.6642 0.0997 0.9374 0.5306 0.0727
		middle	0.8770 0.0182 0.4574 0.7859 0.0624 0.4642
0.55	Ring 1	vertices	0.3346 0.1374 0.5821 0.7156 0.0004 0.0058
		middle	0.9115 0.2610 0.5226 0.5150 0.8907 0.8797
	Ring 2	vertices	0.9880 0 0.7452 0.9712 0.0403 0.3601
		middle	0.2336 0 0.7036 0.9477 0.4303 0.1574
0.60	Ring 1	vertices	0.9884 0.9295 0.0697 0.6940 0.9392 0.0204
		middle	0.9984 0.3378 0.7331 0.9962 0.4149 0.7276
	Ring 2	vertices	0.9175 0.0034 0.8338 0.8661 0.3837 0.0133
		middle	0.3536 0.3297 0.7676 0.9030 0.6372 0.0866

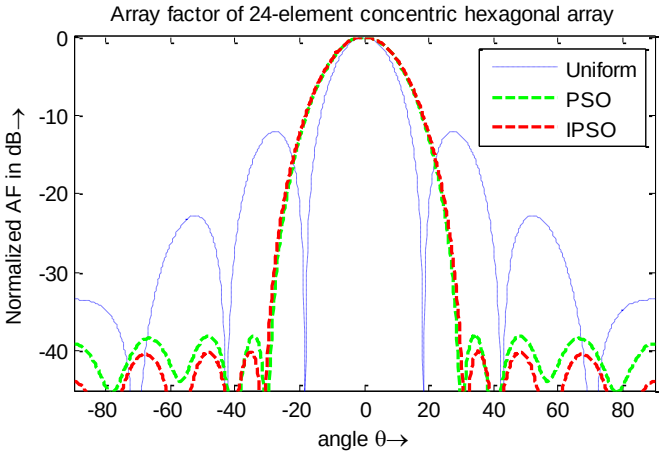

Figure 10. Normalized absolute power patterns of optimized CHA and its corresponding uniformly excited array with fixed inter-ring spacing d_h=0.5λ.

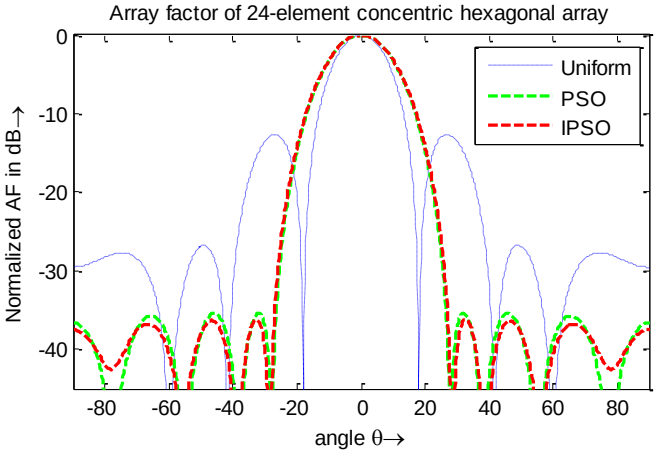

Figure 11. Normalized absolute power patterns of optimized CHA and its corresponding uniformly excited array with fixed inter-ring spacing d_h=0.55λ.

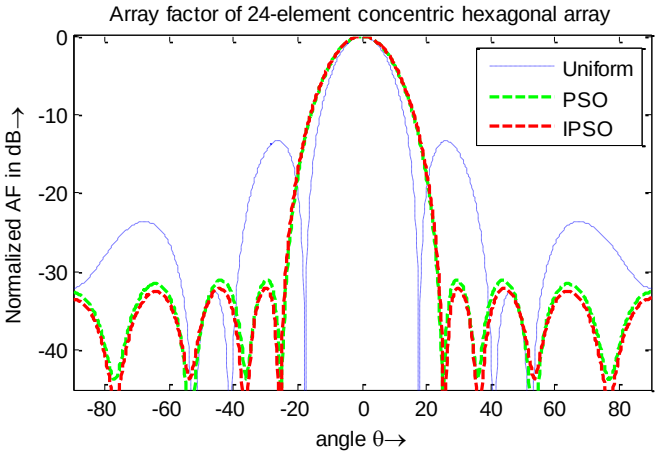

Figure 12. Normalized absolute power patterns of optimized CHA and its corresponding uniformly excited array with fixed inter-ring spacing d_h=0.6λ.

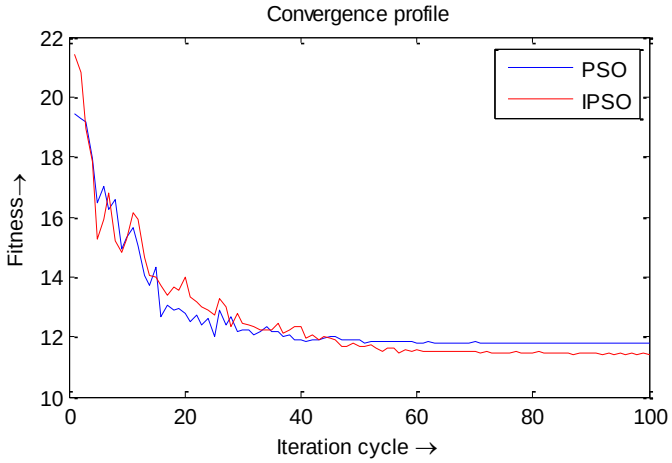

Figure 13. Convergence profiles for the 24-element CHA using PSO and IPSO.

In the third example, optimal design of 30-element CHA with amplitudes only optimization is presented. IPSO technique is used to determine an optimal set of non-uniformly excited array that provides a radiation pattern with maximum SLL reduction.

In this example, CHA of two concentric rings having 12 elements in the inner-ring and 18 elements in the outer-ring is considering for synthesis. Here also three cases are considered for three different values of inter-ring spacing (d_h) along X-axis in the array. In the first case, spacing between hexagons in CHA is 0.5λ. Similarly, for the second and third cases, spacing is 0.55λ and 0.6λ, respectively. The inter-element spacing of the inner ring is kept fixed at d=λ/2 for all the three cases. The value of wave number *k* is chosen 8.373 so that the operating frequency of the array antenna is 400MHZ.

Performances of 30-element amplitudes only optimized array with variation of spacing between hexagons are tabulated in Table VII. The optimal excitation amplitudes for this CHA using PSO and IPSO are shown in Table VIII and Table IX, respectively. Figure 14-16 show the array pattern found by PSO and IPSO for various inter-ring spacing of 30-element CHA and comparison of them with fully populated array pattern.

The population size using each algorithm (PSO and IPSO) by which the antenna array is optimized is 50 and maximum number of iteration cycles is 100. The minimum *CF* values are recorded against number of iteration cycles to get the convergence profiles for each algorithm, which is shown in Figure 17.

Table VII: Performances of 30-element CHA using PSO and IPSO

Inter-ring spacing d_h(λ)	SLL		FNBW	
	PSO	IPSO	PSO	IPSO
0.50	-30.70	-35.56	49.6	53.6
0.55	-25.05	-27.97	41.6	43.6
0.60	-24.41	-26.49	41.2	43.2

Table VIII: Excitation amplitude distribution of 30-element CHA using PSO

Inter-ring spacing d_h(λ)	Ring number	Placement of elements	Amplitude distribution
0.50	Ring 1	vertices	1.0000 0 0 0.7163 0.0000 0
		middle	1.0000 0.4074 1.0000 1.0000 0.5067 1.0000
	Ring 2	vertices	0.3476 0 0.0047 0.4775 0.0782 0
		1st position	0.8775 0 0.3748 0.7105 0 0.3961
		2nd position	0.0001 1.0000 0.8858 0.4726 0.2895 0.0062
0.55	Ring 1	vertices	1.0000 0 0.5700 0.2016 0 1.0000
		middle	1.0000 0 1.0000 1.0000 0 1.0000
	Ring 2	vertices	0.8516 0 0 0.0000 0 0.0118
		1st position	1.0000 0.2395 0 0.9268 0.3235 0
		2nd position	0.4684 0.3296 1.0000 1.0000 0 0
0.60	Ring 1	vertices	0.6938 0.1086 0 0.5902 1.0000 0
		middle	1.0000 0.3518 0.9841 1.0000 0 1.0000
	Ring 2	vertices	0.4473 0 0 1.0000 0 0.1643
		1st position	1.0000 0 0 0 0 1.0000
		2nd position	1.0000 0 0.1887 0.1277 1.0000 0.0471

Table IX: Excitation amplitude distribution of 30-element CHA using IPSO

Inter-ring spacing d_h(λ)	Ring number	Placement of elements	Amplitude distribution
0.50	Ring 1	vertices	0 0.1672 0.0000 0.8771 0.7943 0.0034
		middle	0.9579 0.4388 0.9212 0.9982 0 0.9972
	Ring 2	vertices	1.0000 0 0 1.0000 0.1951 0.0001
		1st position	0.0028 0.0627 0.6266 0.1805 0.0009 0.3946

		2nd position	0 0.5095 0 0 0.4000 0
0.55	Ring 1	vertices	0 0 0.0732 0.3531 0.5021 0
		middle	1.0000 0.4422 1.0000 1.0000 0 1.0000
	Ring 2	vertices	1.0000 0 0 0 0 0.0043
		1st position	0.1870 0 1.0000 0.8873 0 0.3423
		2nd position	0 1.0000 0.9868 0.2982 0.7618 0.9749
0.60	Ring 1	vertices	0 1.0000 0 1.0000 1.0000 0
		middle	1.0000 0 1.0000 1.0000 0 1.0000
	Ring 2	vertices	0 0 0 0.7310 0 0.3053
		1st position	0.5951 0 0 0 0 0.5027
		2nd position	1.0000 0 0 0.0298 0.4134 1.0000

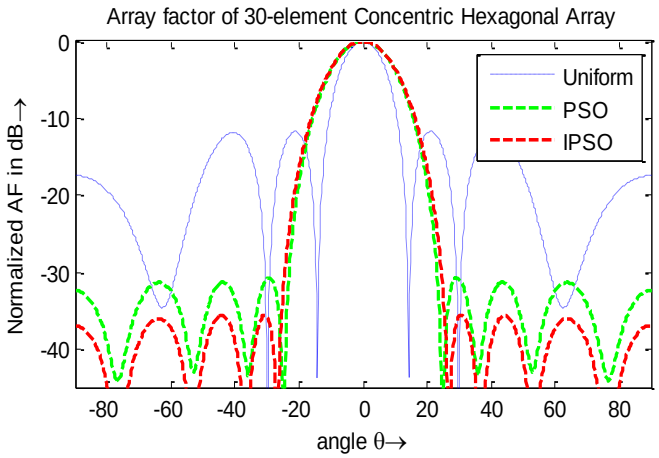

Figure 14. Normalized absolute power patterns of optimized CHA and its corresponding uniformly excited array with fixed inter-ring spacing d_h=0.5λ.

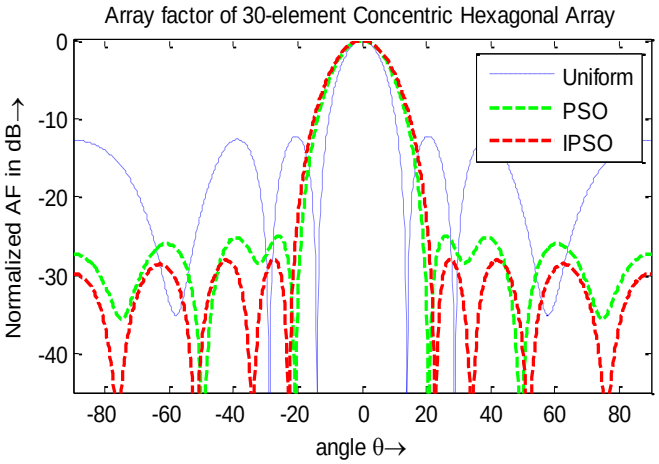

Figure 15. Normalized absolute power patterns of optimized CHA and its corresponding uniformly excited array with fixed inter-ring spacing d_h=0.55λ.

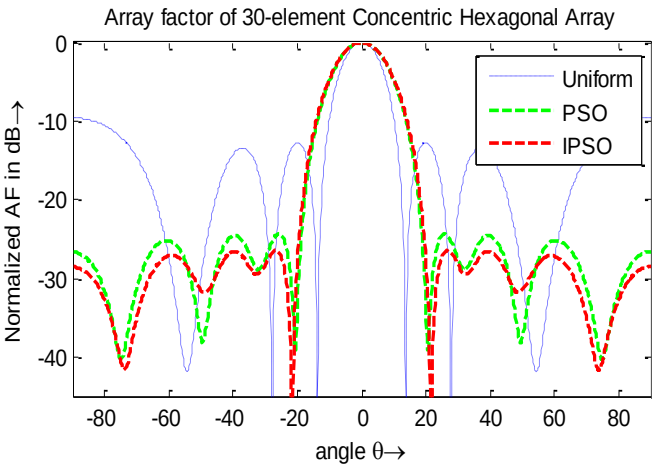

Figure 16. Normalized absolute power patterns of optimized CHA and its corresponding uniformly excited array with fixed inter-ring spacing d_h=0.6λ.

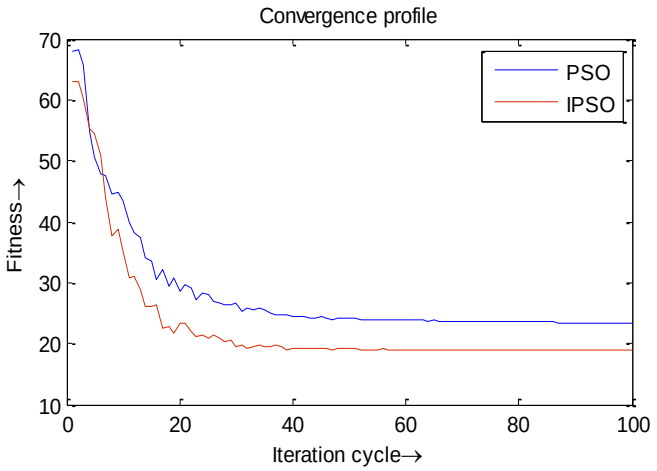

Figure 17. Convergence profile for a 30-element CHA using PSO and IPSO.

V. Conclusions

This paper illustrates the optimal designs of non-uniformly excited CHAs for maximum SLL reduction of radiation patterns. Two evolutionary techniques, PSO and NPSO are applied to achieve the optimal designs. For the first example, the simulation results show that the maximum SLL of antenna array pattern can be brought down from -12.05dB to -20.14dB and -22.96dB using PSO and IPSO, respectively, with simultaneous reduction in number of array elements in the array. Similarly, for the second and third examples, IPSO gives more reduction in SLL compared to PSO. Although, FNBW of the synthesized array pattern using IPSO is slightly greater than the synthesized pattern using PSO. It is of significance to note that although the proposed algorithms are implemented to constrain the synthesis of planar array with isotropic elements, it is not limited to this case only. The proposed algorithms can easily be implemented in non-isotropic element antenna arrays with different geometries to design various array patterns.

References

[1]. C. A. Balanis, *Antenna Theory and Design*, 3rd Edition, John Wiley & Sons, 2005.

[2]. M. Chryssomallis, "Smart antennas," *IEEE Antennas and Propagation Magazine*, vol. 42, no. 3, pp. 129-136, Jun. 2000.

[3]. P. Ioannides and C. A. Balanis, "Uniform circular arrays for smart antennas," *IEEE Antennas and Propagation Magazine*, vol. 47, no. 4, pp. 192-206, Aug. 2005.

[4]. A. A. Lotfi, M. Ghiamy, M. N. Moghaddasi, and R. A. Sadeghzadeh, "An investigation of hybrid elliptical antenna arrays," *IET Microw. Antennas Proag.*, vol. 2, no. 1, pp. 28-34, Jan. 2008.

[5]. M. Dessouky, H. Sharshar, and Y. Albagory, "Efficient sidelobe reduction technique for small - sized concentric circular arrays," *Progress in Electromagnetics Research, PIER*, vol. 65, pp. 187-200, 2006.

[6]. A. Razavi, and K. Forooraghi, "Thinned arrays using pattern search algorithms," *Progress In Electromagnetics Research*, PIER 78, 61-71, 2008.

[7]. L. Schwartzman, "Element behavior in a thinned array," *IEEE Trans. Antennas Propag.*, Vol. 15, No. 7,571-572, 1967.

[8]. R. L. Haupt, "Thinned arrays using genetic algorithms," *IEEE Trans. Antennas Propag.*, Vol. 42, No. 7,993-999, 1994.

[9]. K. Guney and S. Basbug, "Interference suppression of linear antenna arrays by amplitude-only control using a bacterial foraging algorithm," *Progress In Electromagnetics Research*, Vol. 79, 475-497, 2008.

[10]. G. Ram, D. Mandal, R. Kar, S. P. Ghoshal, "Design of Non-uniform Circular Antenna Arrays Using Firefly algorithm for Side Lobe Level Reduction", *International Journal of Electrical and Electronics Engineering*, Vol. 8, No.1, pp. 33-38, 2014.

[11]. K. R. Mahmoud, M. El-Adway, S. M. M. Ibrahem, R. Basnel, R. Mahmoud, and S. H. Zainud-Deen, "A comparition between circular and hexagonal array geometries for smart antenna systems using particle swarm algorithm," *Progress in Electromagnetics Research, PIER*, vol. 72, pp. 75-90, 2007.

[12]. A. Chatterjee and D. Mandal, "Synthesis of hexagonal planar array using swarm-based optimization algorithms", *International Journal of Microwave and Wireless Technologies*, Volume 7, Issue 2, pp 151 – 160, 2015.

[13]. R. Bera and J. S. Roy, "Thinning of elliptical and concentric elliptical antenna arrays using particle swarm optimization," *Microwave Review*, Vol. 19, No. 1, pp. 2-7, September 2013.

[14]. R. C. Eberhart, and Y. Shi, "Particle swarm optimization: Devel- opments, applications and resources,"*Proc. Congr. Evolutionary Computation*, Vol. 1, 81-86, 2001.

[15]. N. Jin and Y. Rahmat-Samii, "Advances in particle swarm optimization for antenna designs: Real-number, binary, single- objective and multiobjective implementations," *IEEE Trans. Antennas Propag.*,Vol. 55, No. 3, 556-567, March 2007.

[16]. J. Kennedy and R. C. Eberhard, "Particle Swarm Optimization," *Proc. of IEEE Int'l Conf. on Neural Networks, Piscataway, NJ, USA*, pp. 1942–1948, 1995.

[17]. Y. Shi, and R. C. Eberhart, "Parameter selection in particle swarm optimization*," in Proc. Seventh Annual Conf. on Evol. Programming*, pp. 591-600, 1998.

[18]. J. Kennedy and R. C. Eberhard, "Particle Swarm Optimization," *Proc. of IEEE Int'l Conf. on Neural Networks, Piscataway, NJ, USA*, pp. 1942–1948, 1995.

[19]. Y. Shi, and R. C. Eberhart, "Parameter selection in particle swarm optimization*," in Proc. Seventh Annual Conf. on Evol. Programming*, pp. 591-600, 1998.

[20]. D. Mandal, S. P. Ghoshal, and A. K. Bhattacharjee, "Improved swarm intelligence based optimal design of concentric circular antenna array," *IEEE Applied Electromagnetics Conference (AEMC 2009)*, pp. 1-4, 2009.

[21]. M. A. Mangoud and H. M. Elragal "Antenna array pattern synthesis and wide null control using enhanced particle swarm Optimization", *Progress In Electromagnetics Research B*, vol. 17, pp. 1-14, 2009.

[22]. S. Mondal, S. P. Ghoshal, R. Kar, D. Mandal, "Linear Phase High Pass FIR Filter Design using Improved Particle Swarm Optimization", *World Academy of Science, Engineering and Technology*, 60, pp. 1621-1627, 2011.

Author Biographies

Rajesh Bera passed B. Tech degree in Electronics and Communication Engineering, from Birbhum Institute of Engineering & Technology, Birbhum, West Bengal, India in the year 2010. He received the M. Tech degree from Kalinga Institute of Industrial Technology, Bhubaneswar, Orissa, India in the year 2012. Presently, he is attached with National Institute of Technology, Durgapur, West Bengal, India, as Institute PhD Research Scholar in the Department of Electronics and Communication Engineering. His research interest includes Array Antenna design; via Evolutionary Computing Techniques.

Durbadal Mandal passed B. E. degree in Electronics and Communication Engineering, from Regional Engineering College, Durgapur, West Bengal, India in the year 1996. He received the M. Tech and Ph. D. degrees from National Institute of Technology, Durgapur, West Bengal, India in the year 2008 and 2011 respectively. Presently, he is attached with National Institute of Technology, Durgapur, West Bengal, India, as Assistant Professor in the Department of Electronics and Communication Engineering. His research interest includes Array Antenna design; filter Optimization via Evolutionary Computing Techniques. He has published more than 230 research papers in International Journals and Conferences.

Sakti Prasad Ghoshal passed B. Sc and B. Tech, degrees in 1973 and 1977, respectively, from Calcutta University, West Bengal, India. He received M. Tech degree from I.I.T (Kharagpur) in 1979. He received Ph.D. degree from Jadavpur University, Kolkata, West Bengal, India in 1992. Presently he is acting as Professor of Electrical Engineering Department of N.I.T. Durgapur, West Bengal, India. His research interest areas are: Application of Evolutionary Computing Techniques to Electrical Power systems, Digital Signal Processing, Array antenna optimization and VLSI. He has published more than 300 research papers in International Journals and Conferences.

Rajib Kar passed B. E. degree in Electronics and Communication Engineering, from Regional Engineering College, Durgapur, West Bengal, India in the year 2001. He received the M. Tech and Ph. D.

degrees from National Institute of Technology, Durgapur, West Bengal, India in the year 2008 and 2011 respectively. Presently, he is attached with National Institute of Technology, Durgapur, West Bengal, India, as Assistant Professor in the Department of Electronics and Communication Engineering. His research interest includes VLSI signal Processing, Filter optimization via Evolutionary Computing Techniques. He has published more than 250 research papers in International Journals and Conferences.